

4-1-2009

# Core-Level Spectroscopy of the Pd/W(110) Interface: Evidence of Long-Range Pd-Island—W Interactions at Submonolayer Coverages

D. Mark Riffe  
*Utah State University*

N. D. Shinn

B. Kim

K. J. Kim

T. H. Kang

Follow this and additional works at: [http://digitalcommons.usu.edu/physics\\_facpub](http://digitalcommons.usu.edu/physics_facpub)



---

## Recommended Citation

"Core-Level Spectroscopy of the Pd/W(110) Interface: Evidence of Long-Range Pd-Island—W Interactions at Submonolayer Coverages," D. M. Riffe, N. D. Shinn, B. Kim, K. J. Kim, and T.-H. Kang, *Surface Science* 603, 1070 (2009) (doi:10.1016/j.susc.2009.02.026).

This Article is brought to you for free and open access by the Physics at DigitalCommons@USU. It has been accepted for inclusion in All Physics Faculty Publications by an authorized administrator of DigitalCommons@USU. For more information, please contact [dylan.burns@usu.edu](mailto:dylan.burns@usu.edu).



# Core-level spectroscopy of the Pd/W(110) interface: Evidence of long-range Pd-island–W interactions at submonolayer Pd coverages

D. M. Riffe <sup>a,\*</sup>, N. D. Shinn <sup>b</sup>, B. Kim <sup>c,d</sup>, K. J. Kim <sup>e</sup>, and T.-H Kang <sup>d</sup>

<sup>a</sup>Physics Department, Utah State University, Logan, UT 84322-4415

<sup>b</sup>Sandia National Laboratories, Albuquerque, NM, 87185, USA

<sup>c</sup>Department of Physics, POSTECH, Pohang, Kyungbuk 790-784, Korea

<sup>d</sup>Beamline Research Division, Pohang Accelerator Laboratory (PAL), Pohang, Kyungbuk 790-784, Korea

<sup>e</sup>Department of Physics, Konkuk University, Seoul 143-701, Korea

(Dated: March 16, 2009)

## Abstract

We have measured W 4f<sub>7/2</sub> core-level photoemission spectra from W(110) in the presence of Pd overayers for coverages up to  $\sim 1$  pseudomorphic monolayer (ML). At coverages close to 0.05 ML a striking change in the W core-level spectrum is observed, which we interpret as indicating a long-range lateral effect of 2D Pd islands upon the W electronic structure in both the first and second W layers. As the coverage increases the long-range effect weakens and finally vanishes near 0.85 ML. Above this coverage the W spectra are typical for a W-based bimetallic interface, with the first-layer W atoms exhibiting a small interfacial core-level shift ( $-95 \pm 5$  meV) compared to the bulk atoms.

**Keywords:** Bimetallic surfaces; Palladium; Soft X-ray photoelectron spectroscopy; Surface electronic structure; Tungsten

\*Corresponding author. Tel.: +1 435 797 3896; fax: +1 435 797 2491. E-mail address: riffe@cc.usu.edu (D. M. Riffe).

## 1. Introduction

The study of bimetallic interfaces has long been driven by the possibility of tailoring surface electronic properties for chemical, catalytic, and electronics applications. Atomic intermixing at the interface can, of course, lead to new and unexpected electronic structure [1, 2]. However, novel surface electronic properties can result in systems with no intermixing. For example, the electronic structure of ultrathin Pd films on transition metal substrates varies systematically with the substrate across the periodic table [2-7]. In fact, for Pd grown on bcc(110) metal surfaces (Nb, Ta, Mo, and W) the electronic structure of monolayer, pseudomorphic Pd most closely resembles that of a noble metal [2, 8-12], leading to surface chemical properties that are very different than those at the surface of bulk Pd [2, 4, 13-24]. Clearly, a surface atom's properties can be substantially influenced by its bonding with the underlying substrate.

Conversely, an ultrathin metallic overlayer can affect the underlying substrate. This is most dramatically illustrated in the phenomenon of overlayer-induced faceting of bcc(111) surfaces (Ta, Mo, and W) [25-36]. Recently, more subtle overlayer-induced effects have been investigated. For example, studies of overlayer mesoscopic islands show that an island can induce substantial elastic strain in the surrounding substrate atoms [37-39]. These island-induced strains can influence adatom diffusion [40, 41], which can subsequently impact island growth and morphology. Overlayer islands can also influence adatom diffusion through their interaction with electrons in substrate surface states [42-44]. These observations naturally raise the following question: can mesoscopic islands produce significant changes in the electronic structure of

the surrounding substrate surface atoms? If so, such an effect might be important to the overall chemical, catalytic, or electronic behavior of the interface.

Here we present evidence that mesoscopic islands can, indeed, significantly alter the electronic structure of nearby substrate surface atoms. Our evidence consists of substantial changes in the core-level spectrum of W(110) upon deposition of very low Pd coverages. The data indicate that the range of the affected W atoms extends  $\sim 1$  nm from the Pd-island edges. Consideration of this range, the magnitude of the core-level shifts ( $\sim 100$  meV), and the coverage dependence of the shifted components leads us to surmise that the Pd islands induce a reconstruction in the region surrounding each island. Furthermore, consideration of earlier very-low-coverage Re/W(110) core-level data [45], which are essentially identical to the data presented here, indicates that this phenomenon is not unique to Pd/W(110); it may thus be a more general phenomenon associated with bimetallic-island formation on W(110) and possibly other bcc(110) surfaces.

## 2. Experimental details

The W 4f<sub>7/2</sub> spectra were obtained using beamline U4A at the National Synchrotron Light Source, which includes a 6-m torodial-grating monochromator and an end station with a 100-mm hemispherical electron-energy analyzer. The data were obtained using 70 eV photons at a total (photon plus electron) energy resolution of  $\sim 125$  meV.

The W crystal was cleaned by the standard technique of sample annealing at 1550 K in an oxygen environment with periodic flashes to 2400 K [46]. As discussed

in detail below, cleanliness is assessed via W  $4f_{7/2}$  photoemission spectra from a freshly flashed sample. We estimate surface contamination to be <1% of a monolayer (ML). The Pd layers were deposited on the room temperature W surface from a shuttered evaporator surrounded by a liquid-nitrogen-cooled shroud. Typical adsorption rates were on the order of 0.05 ML/min.

### 3. Results and analysis

The data in Fig. 1 illustrate the development of the W  $4f_{7/2}$  spectrum with increasing Pd coverage, determined as described in Sec. 4.2. The top curve, from a clean surface, consists of two peaks: the lower binding-energy (BE) peak (surface) is from W atoms in the first atomic layer, and the higher BE peak (bulk) is from W atoms in the second atomic layer and deeper [47, 48]. The solid and dashed vertical lines mark the BE's of the bulk and clean-surface atoms, respectively. At the lowest Pd coverages in our study ( $\sim 0.05$  ML), the spectrum undergoes a remarkable change: both peaks in the spectrum shift to lower binding energy and become significantly broader. This is in marked contrast to the change induced by low coverages of Ni or Pt, for example, which simply cause the low BE peak to decrease in height and move to higher BE [49, 50]. With further coverage, however, the spectrum does becomes more typical of a late transition-metal overlayer on W: the lower BE peak diminishes in size until only one peak is visible [49, 51, 52]. As in the case of Ni deposition on W(110), this single peak is at a slightly lower BE than the bulk peak, indicating that the Pd influenced atoms have a BE that is slightly lower than the bulk-atom BE [49].

We use least-squares fitting to decompose the core-level data into spectral components. Each W  $4f$  core-level photoemission feature is modeled by a Gaussian broadened Doniach-Šunjić (DS) peak [48, 53], which is described by 5 parameters: a Lorentzian width, singularity index, binding energy, peak height, and Gaussian width. We use a linear function to describe the background.

Figure 2a illustrates a least-squares fit to a spectrum from the W(110) surface before Pd deposition. The fit is dominated by two DS components (labeled B and S) that have parameters consistent with data obtained at higher resolution [48]. Additionally, in order to get a satisfactory least-squares fit to the spectrum it is necessary to include two more, much smaller components, as illustrated. As recently discussed in our core-level study of Ni/W(110), the higher binding-energy component is likely from residual C on the surface [49]. Given the size of this peak ( $2.1 \pm 0.2$  % of the surface  $4f_{7/2}$  peak) and the expectation that C sits in the quasi-three-fold hollow site, the contamination is estimated to be <1% of a ML. The small peak that sits between the bulk and surface peaks is possibly due to step-edge atoms on the surface [54, 55].

At lower Pd coverages satisfactory fits to the spectra can only be obtained by adding in two more core-level

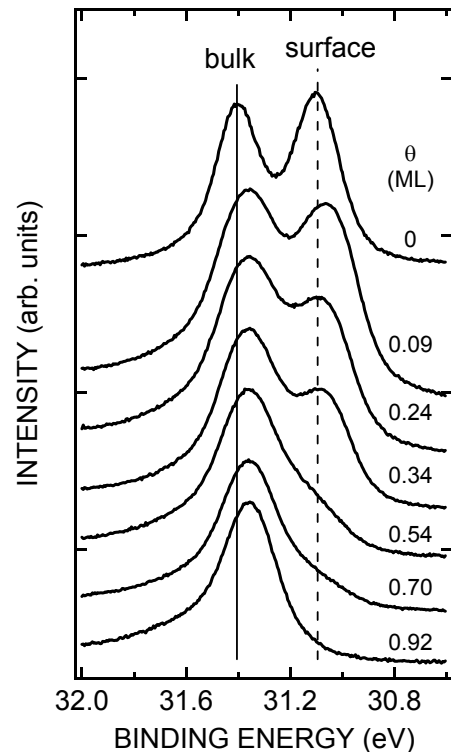


FIG. 1 W $4f_{7/2}$  core-level spectra from the Pd/W(110) bimetallic interface, illustrating the effect of increasing Pd coverage. The solid and dashed lines mark the positions of the bulk and clean-surface core-level features, respectively.

components ( $I_1$  and  $I_2$ ), as illustrated in Fig. 2b-d. The presence of these two components is responsible for the initial shift and broadening of the W  $4f_{7/2}$  spectrum. The need for both of these interfacial components is independent of the exact details of the least-squares analysis.

However, because the Pd induced components are not resolved, it is necessary to limit the number of free parameters in the analysis in order to obtain physically reasonable results over the whole range of Pd coverages. Overall, we initially constrain the fitting parameters to values obtained from clean-surface spectra, and then relax the constraints, as necessary, until a satisfactory fit is obtained. For example, the BE's of the B and S components were initially maintained at their clean-surface value. This constraint is satisfactory at coverages  $<\sim 0.5$  ML, but acceptable fits at higher coverages can only be obtained if the S peak is allowed to move to slightly higher BE, as illustrated in Fig. 2d-f. Similar considerations were applied to the parameters that describe the components' shape. For example, the B and S lines of the clean-surface spectrum have nearly identical Gaussian widths. We thus constrained the Gaussian width of all lines to be identical, and satisfactory fits for all Pd coverages were obtained with this constraint. Because the  $I_1$  and  $I_2$  peaks are associated with first and second

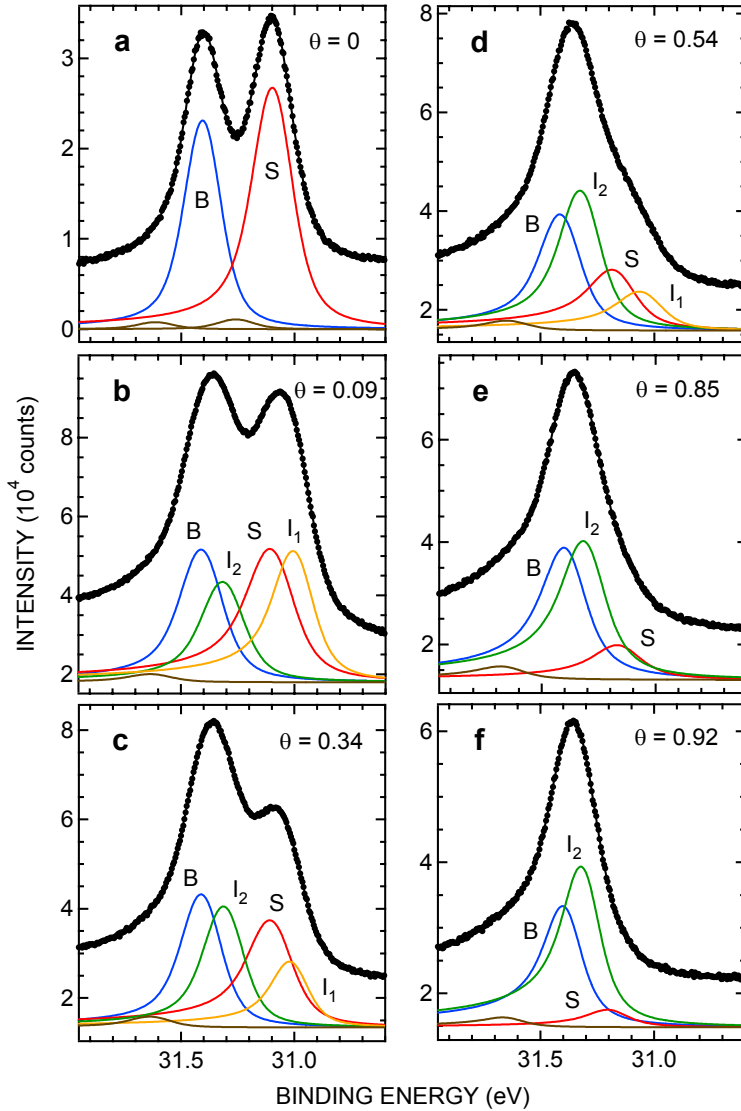


FIG. 2 Least-squares analysis of W  $4f_{7/2}$  core-level spectra from the Pd/W(110) bimetallic interface. Peaks due to bulk W (B), clean-surface W (S), and Pd-induced features ( $I_1$  and  $I_2$ ) are labeled. The origin of the smaller, unlabelled components are discussed in the text. Indicated coverages of Pd are in units of a ps ML.

layer W, respectively (see Sec. 4.1), we also fixed their Lorentzian widths to equal those of the S and B peaks. However, we found that satisfactory fits could only be obtained by allowing the Lorentzian width of the  $I_1$  peak to become slightly smaller. For as-deposited Pd we also found it necessary to allow the singularity index of all of the lines to increase compared to the clean-surface values. This increase can be ascribed to an asymmetric inhomogeneous broadening of the core-level components and/or a Pd induced change in the screening character of the core holes.

With these constraints the least-squares analysis provides the following insights into the spectra from the Pd covered surface. As Fig. 2 illustrates, with increasing Pd coverage (beyond our lowest coverage of  $\sim 0.05$  ML),

the S and  $I_1$  peaks both diminish in size, while the B and  $I_2$  peaks both increase in intensity. At the highest coverages (Fig. 2e-f), only the B, S, and  $I_2$  components are present. As a function of Pd coverage the interfacial core-level shift (ICS) of the  $I_2$  peak is remarkably constant at  $-0.095 \pm 0.005$  eV, while the  $I_1$  ICS decreases slightly, from  $-0.415 \pm 0.005$  eV to  $-0.375 \pm 0.020$  eV, with increasing Pd coverage.<sup>1</sup>

To gain further insight into the Pd spectra, we also

---

<sup>1</sup> The interfacial core-level shift is defined as the difference in binding energy between a Pd influenced core level and the binding energy of bulk W atoms.

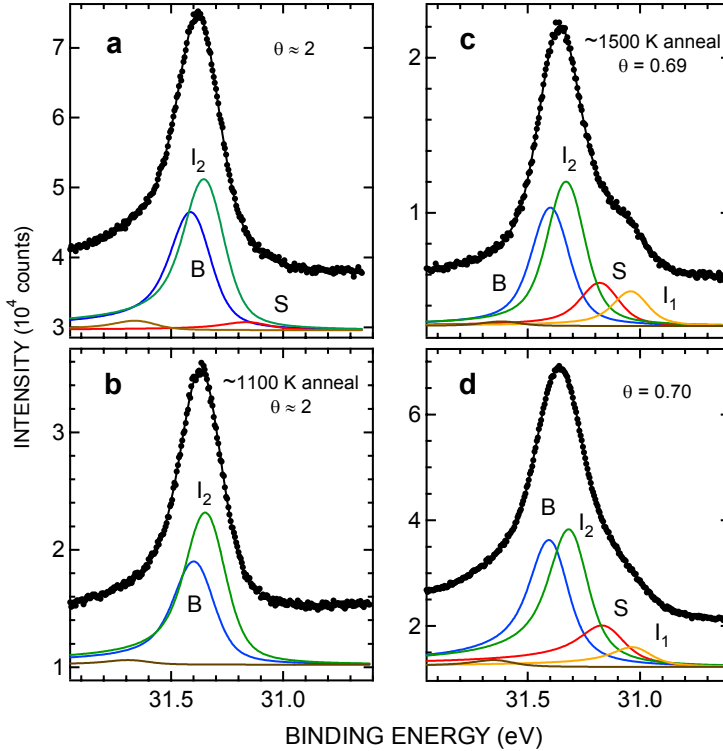


FIG. 3 Comparison of W 4f<sub>7/2</sub> spectra from annealed and unannealed Pd layers. Spectra (a) and (b) are from unannealed and  $\sim 1100$  K annealed interfaces, respectively, with  $\sim 2$  ps ML of Pd. Spectrum (c) is from the surface in (b) further annealed to  $\sim 1500$  K. Spectrum (d) is from a RT-deposited interface at nearly the same coverage as the interface in (c).

collected data from samples that were high-temperature annealed and then recooled to RT. This thermal processing can allow an interface to equilibrate if RT deposition results in a disordered or otherwise metastable interface. Figure 3a-c displays a sequence of spectra from a sample with an initial deposition of  $\sim 2$  ML. The spectrum in Fig. 3a, from the as-deposited interface, mainly consists of the B and I<sub>2</sub> components, plus a very small S contribution. Compared to the sub-ML spectra, the I<sub>2</sub> ICS is somewhat smaller,  $-0.060 \pm 0.010$  eV. Annealing this interface to  $\sim 1100$  K for several seconds, which is sufficient to produce equilibrium but not desorb any Pd [56], results in the nearly identical spectrum shown in Fig. 3b. Compared to the spectrum in Fig. 3a, the peaks are slightly narrower, the S component has vanished, and the I<sub>2</sub> ICS is nearly the same,  $-0.055 \pm 0.010$  eV. Further annealing of this interface to  $\sim 1500$  K, which leaves less than a ML of Pd on the surface, results in the Fig. 3c spectrum, which consists of the B, S, I<sub>1</sub> and I<sub>2</sub> components. For comparison, a spectrum from an as-deposited interface with essentially the same Pd coverage is shown in Fig. 3d. Compared to the spectrum in Fig. 3d, the spectrum in Fig. 3c has slightly narrower peaks, a slight different ratio of S and I<sub>1</sub> intensities, and a perhaps a slightly smaller I<sub>2</sub> ICS ( $-0.085 \pm 0.010$  eV compared to  $-0.095 \pm 0.005$  eV). The observation that the spectra in Fig. 3c and 3d are very similar indicates

that the surface associated with sub-ML, as-adsorbed Pd is not substantially different than the equilibrium surface, at least in terms of atom-specific electronic structure.

## 4. Discussion

### 4.1 Assignments of spectral components

Prior structural work on the Pd/W(110) interface [15, 56-59] is key to understanding the origin of the core-level components in Fig. 2. Submonolayer Pd films deposited at RT grow pseudomorphically, initially as small 2D islands that grow in size and then coalesce as the coverage approaches 1 ML. An unannealed layer, however, shows considerable disorder and a maximum coverage of  $\sim 0.86$  ML before the second layer begins to grow. Layer by layer growth proceeds up to  $\sim 4$  ML. Annealing several layers above 920 K (but at temperatures low enough to prevent desorption) transforms the interface into a single pseudomorphic (ps) Pd layer topped by sparse 3D Pd islands.

We first consider higher coverage data such as that shown in Fig. 2e-f. Because these data show a much reduced S component, they are consistent with a nearly completed ML of Pd. Further, because the S spectral weight has reappeared in the I<sub>2</sub> component, in this coverage range we can assign the I<sub>2</sub> component to first-layer W atoms that are covered by a ps ML of Pd. An *ab initio*

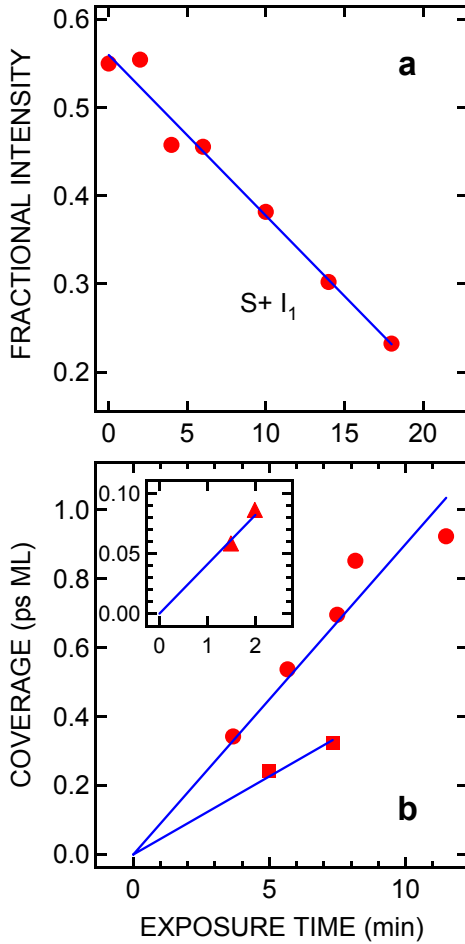


FIG. 4 Fractional intensity of the S+I<sub>1</sub> peaks (a) and Pd coverage (b) as a function Pd exposure time. The three sets of data in (b) are for three different evaporator currents, 9 A (inset), 9.5 A, and 10 A. The solid lines are a linear fits to the data; in (b) the intercept is set equal to zero.

computation supports this assignment. A shift of +0.25 eV in BE of the clean-surface atoms upon deposition of a ps ML of Pd has been calculated [60], which is in good agreement with our experimental values of +0.225 eV for as-deposited Pd and +0.265 eV and +0.235 for the two spectra from the annealed surfaces shown in Fig. 3b-c. Our measured shifts are also in semiquantitative agreement with a model of interfacial core-level shifts based on Born-Haber cycles [61], which we discuss (along with shifts for ps Ni and Pt layers) elsewhere [50].

The fact that Pd forms 2D ps islands at the lowest coverages enables us to assign the Pd induced components in this coverage region. Because of this island formation, the fractional spectral weight from W atoms *not* directly covered by Pd should smoothly decrease with Pd coverage. The S peak by itself does not do this: with initial deposition its intensity decreases dramatically, and then much less slowly with further adsorption. This indicates that some uncovered first-layer W atoms have shifted

core-levels. Two observations immediately suggest that the I<sub>1</sub> component is also from uncovered surface-layer W atoms: the I<sub>1</sub> BE is relatively close to the S component BE, and the I<sub>1</sub> intensity also decreases with increasing Pd deposition. This assignment is confirmed in Fig. 4a, where we have plotted the fractional intensity of the sum of the S and I<sub>1</sub> peaks as a function of exposure time for a set of spectra that were collected at a constant evaporator current. As this figure clearly shows, this combined spectral weight smoothly decreases with Pd coverage. We thus also assign the I<sub>1</sub> peak to uncovered first-layer W atoms. Recognizing that these atoms are (*i*) uncovered and (*ii*) influenced by adsorbed Pd, we conclude that the I<sub>1</sub> atoms are first-layer W atoms in proximity to the Pd islands.

It might seem that we are finished assigning the origins of the I<sub>1</sub> and I<sub>2</sub> components. However, at the lowest exposures the I<sub>2</sub> component is simply too large to be solely due to first-layer W atoms covered by ps Pd islands. This suggests that part of the spectral weight of the I<sub>2</sub> component is also due to some of the second-layer W atoms. Because the Pd islands modify the electronic structure of nearby first-layer atoms (as reflected in the I<sub>1</sub> shift), we surmise that the I<sub>2</sub> component arises from second-layer W atoms directly under the I<sub>1</sub> atoms. With such an assignment, then, versus Pd coverage the I<sub>2</sub> peak goes from becoming predominantly due to W atoms covered by I<sub>1</sub> W atoms to W atoms covered by ps Pd. The assignments of all four spectral components are illustrated in Fig. 5.

#### 4.2 Coverage dependence of component intensities

In this section we develop a model of the coverage dependence of the component intensities that is based upon the spectral assignments in Fig. 5. This model will allow us not only to assign a Pd coverage to each spectrum, but also allow us to confirm that the assignments in Fig. 5 are consistent with the coverage-dependent intensities of all four core-level components.

Based upon the identifications illustrated in Fig. 5 for the different core-level components, we propose the following model for the spectral weights (i.e., integrated intensities) of the components:

$$W_S = W_{S0} (1 - \theta - \theta_1), \quad (1a)$$

$$W_1 = W_{S0} \theta_1, \quad (1b)$$

$$W_2 = W_{S0} x\theta + W_{B0}\theta_1, \quad (1c)$$

$$\begin{aligned} W_B = & (1 - W_{S0}) (1 - \theta - \theta_1) \\ & + (1 - W_{S0} - W_{B0}) \theta_1 \\ & + (1 - W_{S0}) x\theta. \end{aligned} \quad (1d)$$

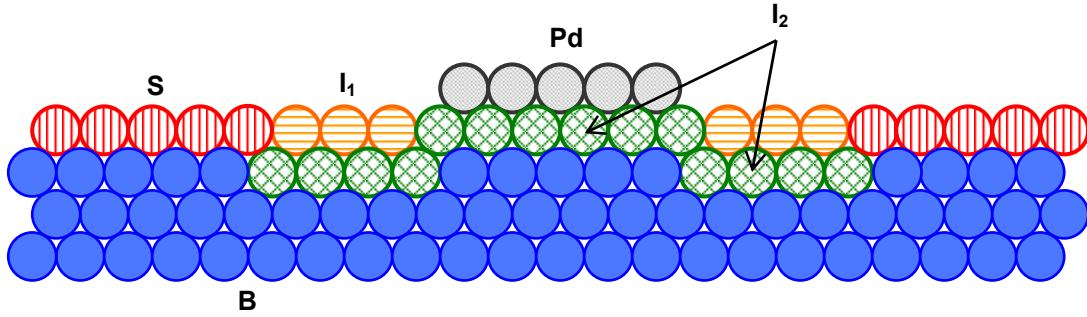


FIG. 5 Assignments of the origins of W 4f<sub>7/2</sub> core-level features B, S, I<sub>1</sub>, and I<sub>2</sub> for submonolayer Pd on W(110). See text for details.

Here  $W_S$ ,  $W_1$ ,  $W_2$ , and  $W_B$  are the spectral weights of the S, I<sub>1</sub>, I<sub>2</sub>, and B components, respectively,  $\theta$  is the Pd coverage,  $\theta_1$  is the coverage of the I<sub>1</sub> atoms,  $W_{S0}$  is the spectral weight for a full monolayer of clean-surface atoms,  $W_{B0}$  is the spectral weight that the second-layer W atoms under the I<sub>1</sub> atoms would have if the surface were totally covered with I<sub>1</sub> atoms, and  $x$  is a factor that accounts for the effect of the Pd layer on the intensities of the W atoms under the Pd layer. In order to keep the number of parameters to a minimum, the model contains several simplifications. First, the factor  $x$  is assumed to be the same for all W atoms below the Pd layer. Second, the model assumes that an I<sub>1</sub> atom has the same spectral weight as an S atom. From Eq. (1) the total spectral weight is calculated to be

$$W_T = 1 - (1 - x) \theta, \quad (2)$$

which shows that the weights in Eq. (1) are normalized so that  $W_T = 1$  at zero coverage. For  $\theta = 1$  (corresponding to a full ML of Pd) Eq. (2) yields  $W_T = x$ , which reflects the effect of the adsorbed Pd layer on the W core-level intensities. From the overall intensities of our spectra we deduce that  $x = 0.7$ . We note that  $x = 0.7$  is consistent with a reduction in intensity arising from inelastic scattering within the Pd layer with an inelastic mean free path (IMFP) of  $\sim 0.6$  nm, which is comparable to the IMFP in bulk Pd [62]. From the fit to the clean-surface data in Fig. 2 we obtain  $W_{S0} = 0.60$ .<sup>2</sup>

The sum of the surface and I<sub>1</sub> intensities can be used to deduce the Pd coverage: summing Eqs. (1a) and (1b), and solving for  $\theta$  yields

$$\theta = 1 - \frac{W_S + W_1}{W_{S0}}. \quad (3)$$

<sup>2</sup> We note that  $W_{S0} \approx 0.55$  is slightly smaller for the set of spectra that were used to produce Fig. 4a.

In order to obtain the normalized weights  $W_S$  and  $W_1$  from our data we must divide the measured weight by the incident beam flux. Unfortunately, there is some systematic error associated with this normalization. This error arises from photoelectron-diffraction induced variations in the overall intensity due to slight angular variations in sample position from run to run. Because of this, we find it slightly more accurate to calculate the coverage from spectral weights that are instead normalized by the total weight of each spectrum. In the model represented by Eq. (1) these fractional intensities  $F_S$ ,  $F_1$ ,  $F_2$ , and  $F_B$  (whose sum is always equal to 1) are obtained from the weights  $W_S$ ,  $W_1$ ,  $W_2$ , and  $W_B$  by dividing by  $W_T$ . The coverage can then be obtained from

$$\theta = \frac{W_{S0} - (F_S + F_1)}{W_{S0} - (F_S + F_1)(1 - x)}. \quad (4)$$

As a check that Eq. (4) yields reasonable results, we compare the coverages calculated via Eq. (4) with the exposure times for the set of data fit in Fig. 2 (along with other data from the same sequence of exposures). This comparison, shown in Fig. 4b, demonstrates that for a given evaporator current the coverage determined by Eq. (4) is proportional to the exposure time, as expected. From the fits in Fig. 4b we determine that the adsorption rates range between 0.04 and 0.09 ML/min.

In Fig. 6a we plot the experimental fractional intensities as a function of the coverage. As the figure shows, both the B and S intensities dramatically drop with the initial  $\sim 0.05$  ML of Pd. Above this coverage the intensity of each component varies approximately linearly vs  $\theta$  up to  $\sim 0.85$  ML, after which the I<sub>1</sub> intensity is zero, the B intensity is approximately constant, and the S and I<sub>2</sub> intensities change at a slightly increased rate. The lines between  $\theta = 0.06$  and 0.85 ML are either linear or quadratic fits to the data.

In order to use the model described by Eq. (1) to calculate coverage-dependent intensities, we need a description of  $\theta_1$  as a function of  $\theta$ . We can obtain this by noting that (i) experimentally  $F_1$  varies approximately linearly vs  $\theta$ ,

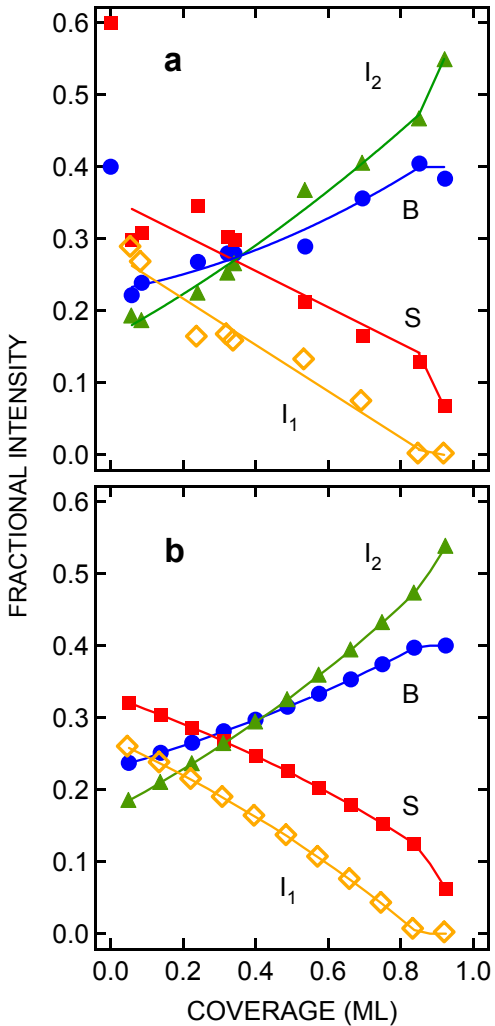


FIG. 6 Measured (a) and model (b) fractional intensities of the B, S, I<sub>1</sub>, and I<sub>2</sub> core-level features vs Pd coverage. The solid lines in (a) are guides to the eye.

and (ii) in the model  $F_1$  varies approximately linearly with  $W_1$ , which is proportional to  $\theta_1$ . We thus write, for  $\theta > 0.05$  (approximately our lowest coverage),

$$\theta_1 = (0.45 - 0.53\theta)\Theta(0.85 - \theta), \quad (5)$$

where  $\Theta$  is the Heaviside function, and the constants 0.45 and 0.53 are determined by the conditions  $F_1(0.05) = 0.26$  and  $F_1(0.85) = 0$ , which are extracted from the linear fit to the I<sub>1</sub> data in Fig. 6a.

In Fig. 6b we plot the fractional intensities  $F_S$ ,  $F_1$ , and  $F_B$  calculated using Eqs. (1), (2), and (5). The only adjustable parameter in the calculation is  $W_{B0}$ , which has been adjusted to 0.38 to provide agreement with the measured data in Fig. 6a. In an escape-depth model of component intensities (based on the ratio of S and B intensities from the clean surface) we would have  $W_{B0} = 0.24$ . Apparently, however, diffraction

of the outgoing electrons causes the layer-dependent intensities to vary somewhat from a simple escape-depth description. This is not uncommon for 4f<sub>7/2</sub> photoemission from W(110) [63, 64]. The overall good agreement between Fig. 6a and Fig. 6b indicates that our assignments of the I<sub>1</sub> and I<sub>2</sub> components are physically realistic.

#### 4.3 Pd-island—W interactions

As we now show, the Pd islands affect the nearby W atoms over a range that is significantly larger than nearest-neighbor (NN) distances. From our model of the component intensities we can obtain a semiquantitative assessment of the size of the regions that produce the I<sub>1</sub> component. Using Eq. (5) we estimate the I<sub>1</sub> coverage to be  $\theta_1 = 0.42$  ML at  $\theta = 0.05$  ML. Under the simplifying assumptions of circular islands and circular I<sub>1</sub> annuli surrounding the islands, this value of  $\theta_1$  implies that the ratio of inner and outer radii of the annuli is  $\sim 3$ . In order to estimate the actual difference in these two radii (and thus the distance over which the Pd islands affect uncovered W atoms), we need to know the island density. Scanning tunneling microscopy (STM) measurements of two similar systems at submonolayer coverages, Ni/W(110) [65] and Fe/Mo(110) [66], show island densities of  $3 \times 10^{12}$  cm<sup>-2</sup> and  $9 \times 10^{12}$  cm<sup>-2</sup>, respectively. For our estimation we use the average value of  $6 \times 10^{12}$  cm<sup>-2</sup>. This density implies an average island radius of  $\sim 0.5$  nm at  $\theta = 0.05$ , which then implies that the difference in inner and outer radii of the I<sub>1</sub> annuli is  $\sim 1$  nm. This distance is equivalent to  $\sim 3a_0$ , where  $a_0 = 0.316$  nm is the W lattice constant.

Such a long-range effect on the W core-levels is quite surprising. In nearly every case of transition-metal deposition on W(110), including Cr [67], Ni [49, 51], Pt [50, 51], and Re [45], the core-level spectra have been interpreted solely in terms of a NN influence of the ad-layer atoms on the W atoms. Similarly, on W(111) and W(211) submonolayer Ru deposition also produces core-level spectra that are consistent with only nearest-neighbor W atoms being affected [68].

In addition to the present case of Pd/W(110) there is one other clearly identified exception to NN-only induced core-level shifts. Core-level data from Fe/W(110) near a ps ML show that the overlayer of Fe perturbs the second W layer, producing an ICS of  $-87 \pm 3$  meV (in addition to the first-layer ICS of  $-231 \pm 5$  meV) [51, 64, 69]. It was speculated that this next-nearest-neighbor shift is the result of the Fe layer inducing a change in relaxation of the near-surface W layers, which produces the core-level shift of the second-layer W atoms [69]. This explanation is supported by several *ab initio* structure calculations of the Fe/W(110) interface, all of which indicate an outward displacement ( $+3.3 \pm 0.2\%$  [70],  $+4.0\%$  [71],  $+4.6\%$  [72]) of the first-layer W atoms upon deposition of a ps Fe ML. Photoelectron-diffraction [64] and X-ray-diffraction [73] measurements are consistent with the theoretically calculated values. Still, in this case the second W layer is only  $\sim 1$  W lattice constant away from

the adsorbed Fe layer.

However, the low-coverage behavior that we observe does not appear to be unique: the Re/W(110) system exhibits submonolayer core-level spectra that are strikingly similar to our Pd/W(110) spectra [45]. Initial ( $\sim 0.1$  ML) Re deposition also produces two other substantial core-level components, with ICS's of  $\sim -0.40$  eV and  $\sim -0.13$  eV. These two shifts are very close to the shifts that we have determined for the  $I_1$  and  $I_2$  components.

Because the low-coverage spectra from Re/W(110) and Pd/W(110) are essentially identical, we posit that the Re/W(110) spectra are due to the same island-induced, long-range mechanism as occurs at the Pd/W(110) interface. We now consider this hypothesis in opposition to the idea put forward by the authors of the Re/W(110) study, that the two low-coverage components are due to intermixing of the Re and W atoms at the interface via a place-exchange mechanism [45].<sup>3</sup> Structural work on the Re/W(110) system supports the new hypothesis. Field ion microscopy (FIM) studies (which have been used extensively to study place exchange on fcc(100) surfaces [74-78], for example), show no indication of place exchange between adsorbed Re and surface W(110) atoms [79-88]. Furthermore, the FIM studies clearly show Re island formation at low coverages [84] near the sample temperature ( $\sim 500$  K) used in the Re core-level studies [45]. Beyond these specific studies, as far as we have been able to ascertain there is no indication in the literature of place exchange between any adsorbed species and W(110) surface atoms for a sample temperature  $<\sim 500$  K. In fact, in a recent theoretical study of Fe/W(110) the likelihood of place exchange during Fe diffusion was investigated and determined to be energetically prohibitive [72]. We also note that in a study of Pd/Mo(110), place exchange between the Pd and surface Mo atoms was explicitly ruled out for a Pd monolayer film annealed up to the Pd desorption temperature [89]. Given that W(110) has a larger surface free energy than Mo(110), this also excludes the possibility of place exchange in the Pd/W(110) system, consistent with the structural studies of Pd/W(110) [15, 56-59]. Furthermore, for both Pd/W(110) and Re/W(110) it appears impossible to reconcile the size of the two shifted core-level peaks with a direct (NN) Re-W interaction at such low adsorbate coverages. We thus conclude that the same mechanism – long-range island-induced shifts – operates in both systems to produce the two low-coverage interfacial core-level peaks.

So what is the specific mechanism that gives rise to this long-range lateral effect in the Pd/W(110) and Re/W(110) systems? Without more detailed structural information than is currently available we cannot con-

clusively answer this question. However, results from other metallic epitaxial systems do allow us to speculate about these two systems. In general, long-range interactions at surfaces are typically divided into two categories: those due to elastic forces and those due to indirect electronic interactions [90]. Elastic interactions occur when an adsorbate atom (or island) perturbs the positions of the surrounding surface atoms. Indeed, the second-W-layer shifts observed in the Fe/W(110) system [69] can be thought of as arising from adsorbate-induced elastic forces that change the position of the first-layer W atoms. Indirect electronic forces between atoms or collections of atoms are mediated via substrate electrons. For atoms on a surface these interactions tend to be more long-ranged than elastic forces and can extend over several nanometers [90].

We now consider whether either of these two effects could possibly produce the observed core-level shifts associated with the  $I_1$  and  $I_2$  features. In our discussion we focus on two quantities pertinent to the core-level shifts: the magnitude and range of the interactions.

Given that Pd and Re have bulk NN distances (0.2752 and 0.2742 nm, respectively) that are almost identical to that for W (0.2740 nm), one might infer that elastic effects would be minimal for these two systems. However, recent *ab initio* calculations of the structure of mesoscale islands in several systems with minimal bulk strain, specifically Co/Cu(100) [37, 40], Co/Cu(111) [41], and Cu/Cu(111) [38], show that bulk-strain considerations are insufficient to understand the physics associated with low-coverage islands. Experimental stress measurements of Fe and Ni overlayers on W(110) confirm this idea [91, 92]. In particular, the theoretical work has shown that the stresses and resulting strains produced in and by mesoscopic islands are very different from those produced by near-ML films. The calculations indicate that significant strain is induced laterally up to  $\sim 0.4$  nm from the edge of a mesoscopic island. Unfortunately, this range is not large enough to explain our results. Additionally, typical energies associated with purely elastic effects are not large enough to explain the magnitude of the observed core-level shifts [93]. Thus, an explanation based on similar elastic effects seems unlikely.

Long-range indirect electronic interactions at the W(110) surface are well documented. Field ion microscopy (FIM) studies of the interactions between metallic adatoms, including Re-Re [80, 82, 85, 88], W-Pd [81, 87], Re-Pd [86, 87], Pd-Pd [94], and Ir-Ir pairs [86, 88, 94], show that the adatoms can interact over distances up to  $\sim 1.3$  nm. Interestingly, for Pd-Pd, Re-Re, and Ir-Ir pairs there exists a similar potential-energy well with a minimum of  $-25$  to  $-30$  meV at  $\sim 1$  nm separation along the  $[1\bar{1}0]$  direction [94]. Whether these long-range interactions include significant elastic contributions or are purely electronic in nature is not known, although the typically small size of purely elastic interactions [93] and the recent observation of charge-density standing waves associated with a W(110) surface-state [95] suggests that

---

<sup>3</sup> The  $-0.40$  eV peak was ascribed to single W atoms that sit above the first W layer, while the  $-0.13$  eV peak was ascribed to first layer W atoms that have a neighboring Re atom that has been incorporated in the first W layer.

an indirect interaction mediated by this surface state [90, 96] may dominate the interactions between atoms at this surface.

In the case of a Pd island indirectly interacting with a surface or second-layer W atom, the substantial number of Pd atoms ( $\sim 15$  atoms per island at  $\theta = 0.05$  ML) would necessarily increase the interaction strength above that of a single pair of atoms, perhaps sufficiently to produce core-level shifts of the magnitude (100 meV) that we observe here. Because electrons in an intrinsic surface state do not scatter from the ground-state W atoms, the contribution of this type of interaction would be a final-state effect in which the Pd atoms interact with a core-excited W atom (which, in the equivalent-cores approximation [97], is equivalent to a Re impurity). The fact that the interacting (impurity) atom is embedded in the surface (or second) W layer might also increase the size of the interaction compared to an atom sitting on top of the W surface. However, given the oscillatory nature of indirect electronic interactions, it is hard to imagine how this mechanism could produce the same core-level shift in all atoms within a 1 nm annulus around each island. In contrast, we expect that such a mechanism would produce a distribution of core-level shifts, which we do not observe.

There is, fortunately, another possible explanation for the Pd-island induced core-level shifts: it is conceivable that island-induced stresses trigger a reconstruction in the nearby surface region. (While one might technically classify an induced reconstruction as an elastic effect, it would not be a typical elastic effect in which the strength of the interaction smoothly falls off with distance.) Because surface reconstruction involves changes in surface-atom bonding, it can have a substantial influence on core-level BE's. For example, the clean W(100) surface exhibits a  $c(2\times 2)$  reconstructed phase that is removed upon saturated H adsorption [98]. The core-level shifts between these two states of the W(100) surface have been attributed to a combination of H chemisorption ( $\sim +110$  meV) and reconstruction ( $\sim -130$  meV) [99]. A reconstruction of the nearby surface region thus offers a plausible explanation for the substantial and uniform core-level shifts of both the first- and second-layer W atoms. The coverage dependence of the  $I_1$  fractional intensity is also at least qualitatively consistent with a reconstruction-based explanation: as the island edges become closer together the stresses in the regions between two islands would be expected to balance each other, thus reducing the range of reconstruction around a given island. Although there is minimal structural evidence for adsorbate-induced reconstruction on W(110), a recent x-ray diffraction study of the  $7\times 1$  closed-packed commensurate phase of Ni/W(110) has inferred substantial displacements (up to  $\sim 0.05$  nm) of the underlying W atoms [100]. The possible contribution of these displacements to the Ni-atom induced core-level shifts at this interface has been previously discussed [49]. The two present

examples of a possible reconstruction, Pd/W(110) and Re/W(110), are different than Ni/W(110) in that the reconstruction is induced in a region that is lateral to, rather than underneath, the overlayer islands.

## 5. Summary and conclusions

In summary, we have measured W  $4f_{7/2}$  core-level binding energies upon submonolayer growth of the Pd/W(110) interface. Two large, Pd-island-induced core-level features are observed at Pd coverages as low as  $\sim 0.05$  ML. The disproportionate intensity of these two components at low coverage shows that they cannot be associated with W atoms in direct contact with the Pd atoms, but are due to an indirect influence of the Pd islands upon the nearby surface region. Elastic effects, indirect surface-state mediated interactions, and island-triggered reconstruction have been considered as potential explanations for the observed shifts. Of the three, island-induced reconstruction can most easily account for (i) uniform shifts in a large region around each island, (ii) significant shifts of both first and second-layer W atoms, and (iii) the coverage dependence of the intensity associated with the first-layer W atoms. Furthermore, consideration of Re-induced shifts on W(110), which at low coverages are nearly identical to those observed for Pd/W(110), indicates that this behavior is not unique to the Pd/W(110) interface, but may represent a more general response of a surface to submonolayer island formation.

There are at least two potential consequences of such an island-induced reconstruction. First, because the  $\sim 100$  meV shift in the core-levels is reflective of a similar shift in the W surface-atom 5d (valence) band [101], the chemical behavior of the surface may be modified. Such modification is probably rather subtle, however: by comparison, the substantial 0.85 eV shift of the Pd  $3d_{5/2}$  core level between the Pd(100) surface and monolayer Pd/W(110) [18] is indicative of the substantial shift in the Pd 4d band that is responsible for the very different Pd chemistry of these two surfaces. Second, the energy barriers for diffusion on a reconstructed region would likely be different than on the unreconstructed surface. This could impact the subsequent growth and morphology of the Pd/W(110) monolayer film, and might be responsible, at least in part, for the large disorder in room-temperature grown films [56].

## Acknowledgments

This work was supported, in part, by the U.S. Department of Energy, Office of Basic Energy Sciences. Sandia National Laboratories is a multi-program laboratory operated by Sandia Corporation, a Lockheed-Martin Company, for the U. S. Department of Energy under Contract No. DE-AC04-94AL85000.

## References

- [1] C. T. Campbell, Annu. Rev. Phys. Chem. 41 (1990) 735.
- [2] J. Rodriguez, Surface Science Reports 24 (1996) 223.

- [3] J. A. Rodriguez, R. A. Campbell, and D. W. Goodman, *J. Phys. Chem.* 95 (1991) 5716.
- [4] J. A. Rodriguez and D. W. Goodman, *Science* 257 (1992) 897.
- [5] J. Rodriguez, *Surf. Sci.* 345 (1996) 347.
- [6] A. Ruban, B. Hammer, P. Stoltze, H. L. Skriver, and J. K. Nørskov, *Journal of Molecular Catalysis A: Chemical* 115 (1997) 421.
- [7] L. A. Kibler, A. M. El-Aziz, R. Hoyer, and D. M. Kolb, *Angew. Chem. Int. Ed.* 44 (2005) 2080.
- [8] M. El-Batanouny, M. Strongin, G. P. Williams, and J. Colbert, *Phys. Rev. Lett.* 46 (1981) 269.
- [9] M. El-Batanouny, D. R. Hamann, S. R. Chubb, and J. W. Davenport, *Phys. Rev. B* 27 (1983) 2575.
- [10] M. W. Ruckman, V. Murgai, and M. Strongin, *Phys. Rev. B* 34 (1986) 6759.
- [11] G. W. Graham, *J. Vac. Sci. Technol. A* 4 (1986) 760.
- [12] M. W. Ruckman and M. Strongin, *Accounts of Chemical Research* 27 (1994) 250.
- [13] M. W. Ruckman and M. Strongin, *Phys. Rev. B* 29 (1984) 7105.
- [14] M. W. Ruckman, P. D. Johnson, and M. Strongin, *Phys. Rev. B* 31 (1985) 3405.
- [15] P. J. Berlowitz and D. W. Goodman, *Langmuir* 4 (1988) 1091.
- [16] B. E. Koel, R. J. Smith, and P. J. Berlowitz, *Surf. Sci.* 231 (1990) 325.
- [17] J. A. Rodriguez, R. A. Campbell, and D. W. Goodman, *J. Phys. Chem.* 94 (1990) 6936.
- [18] R. A. Campbell, J. A. Rodriguez, and D. W. Goodman, *Surf. Sci.* 240 (1990) 71.
- [19] A. Sellidj and B. E. Koel, *Surf. Sci.* 284 (1993) 139.
- [20] Y.-W. Yang, J. C. Lin, and T. Engel, *Surf. Sci.* 289 (1993) 267.
- [21] W. K. Kuhn, J. Szanyi, and D. W. Goodman, *Surf. Sci.* 303 (1994) 377.
- [22] C. Xu and D. W. Goodman, *Langmuir* 12 (1996) 1807.
- [23] C. Xu and D. W. Goodman, *J. Phys. Chem.* 100 (1996) 245.
- [24] D. E. Beck, J. M. Heitzinger, A. Avoyan, and B. E. Koel, *Surf. Sci.* 491 (2001) 48.
- [25] K.-J. Song, R. A. Demmin, C. Dong, E. Garfunkel, and T. E. Madey, *Surf. Sci.* 227 (1990) L79.
- [26] T. E. Madey, K.-J. Song, C.-Z. Dong, and R. A. Demmin, *Surf. Sci.* 247 (1991) 175.
- [27] T. E. Madey, J. Guan, D. Cheng-Zhi, and S. M. Shivaprasad, *Surf. Sci.* 287-288 (1993) 826.
- [28] K.-J. Song, J. C. Lin, M. Y. Lai, and Y. L. Wang, *Surf. Sci.* 327 (1995) 17.
- [29] J. Guan, R. A. Campbell, and T. E. Madey, *Surf. Sci.* 341 (1995) 311.
- [30] J. Guan, R. A. Campbell, and T. E. Madey, *J. Vac. Sci. Technol. A* 13 (1995) 1484.
- [31] C.-H. Nien and T. E. Madey, *Surf. Sci.* 380 (1997) L527.
- [32] T. E. Madey, C.-H. Nien, K. Pelhos, J. J. Kolodziej, I. M. Abdelrehim, and H.-S. Tao, *Surf. Sci.* 438 (1999) 191.
- [33] C.-H. Nien, T. E. Madey, Y. W. Tai, T. C. Leung, J. G. Che, and C. T. Chan, *Phys. Rev. B* 59 (1999) 10335.
- [34] R. Szukiewicz and J. Kolaczkiewicz, *Surf. Sci.* 547 (2003) L837.
- [35] D. B. Danko, M. Kuchowicz, and J. Kolaczkiewicz, *Surf. Sci.* 552 (2004) 111.
- [36] Y. W. Liao, L. H. Chen, K. C. Kao, C. H. Nien, M. T. Lin, and K. J. Song, *Phys. Rev. B* 75 (2007) 125428.
- [37] V. S. Stepanyuk, D. I. Bazhanov, A. N. Baranov, W. Hergert, P. H. Dederichs, and J. Kirschner, *Phys. Rev. B* 62 (2000) 15398.
- [38] O. V. Lysenko, V. S. Stepanyuk, W. Hergert, and J. Kirschner, *Phys. Rev. Lett.* 89 (2002) 126102.
- [39] O. Mironets, H. L. Meyerheim, C. Tusche, V. S. Stepanyuk, E. Soyka, P. Zschack, H. Hong, N. Jeutter, R. Felici, and J. Kirschner, *Phys. Rev. Lett.* 100 (2008) 096103.
- [40] V. S. Stepanyuk, D. I. Bazhanov, W. Hergert, and J. Kirschner, *Phys. Rev. B* 63 (2001) 153406.
- [41] D. V. Tsivlin, V. S. Stepanyuk, W. Hergert, and J. Kirschner, *Phys. Rev. B* 68 (2003) 205411.
- [42] A. Bogicevic, S. Ovesson, P. Hyldgaard, B. I. Lundqvist, H. Brune, and D. R. Jennison, *Phys. Rev. Lett.* 85 (2000) 1910.
- [43] K. A. Fichthorn, M. L. Merrick, and M. Scheffler, *Phys. Rev. B* 68 (2003) 041404.
- [44] S. U. Nanayakkara, E. C. H. Sykes, L. C. Fernandez-Torres, M. M. Blake, and P. S. Weiss, *Phys. Rev. Lett.* 98 (2007) 206108.
- [45] N. T. Barrett, B. Villette, A. Senhaji, C. Guillot, R. Belkhou, G. Tréglia, and B. Legrand, *Surf. Sci.* 286 (1993) 150.
- [46] R. G. Musket, W. McLean, C. A. Colmenares, D. M. Makowiecki, and W. J. Siekhaus, *Applications of Surface Science* 10 (1982) 143.
- [47] T. M. Duc, C. Guillot, Y. Lassailly, J. Lecante, Y. Jugnet, and J. C. Vedrine, *Phys. Rev. Lett.* 43 (1979) 789.
- [48] D. M. Riffe, G. K. Wertheim, and P. H. Citrin, *Phys. Rev. Lett.* 63 (1989) 1976.
- [49] D. M. Riffe, R. T. Franckowiak, N. D. Shinn, B. Kim, K. J. Kim, and T.-H. Kang, *Surf. Sci.* 602 (2008) 2039.
- [50] D. M. Riffe, N. D. Shinn, B. Kim, K. J. Kim, and T.-H. Kang, in preparation.
- [51] N. D. Shinn, B. Kim, A. B. Andrews, J. L. Erskine, K. J. Kim, and T.-H. Kang, *Material Research Society Symposium Proceedings* 307 (1993) 167.
- [52] H.-S. Tao, J. E. Rowe, and T. E. Madey, *Surf. Sci.* 407 (1998) L640.
- [53] S. Doniach and M. Šunjic, *J. Phys. C: Solid State Phys.* 34 (1970) 285.
- [54] D. M. Riffe, B. Kim, and J. L. Erskine, *Phys. Rev. B* 50 (1994) 14481.
- [55] C. Zilkens, *Gestufte Oberflächen und Quasieindimensionale Strukturen Photoemission an 3d Metallen auf W(110)*, University of Köln (2002).
- [56] W. Schlenk and E. Bauer, *Surf. Sci.* 93 (1980) 9.
- [57] D. W. Bassett, *Thin Solid Films* 48 (1978) 237.
- [58] J. Kolaczkiewicz and E. Bauer, *Surf. Sci.* 151 (1985) 333.
- [59] J. Kolaczkiewicz and E. Bauer, *Surf. Sci.* 256 (1991) 87.
- [60] R. Wu and R. R. Freeman, *Phys. Rev. B* 32 (1995) 12419.
- [61] A. Nilsson, B. Eriksson, N. Mårtensson, J. N. Andersen, and J. Onsgaard, *Phys. Rev. B* 38 (1988) 10357.
- [62] S. Tanuma, C. J. Powell, and D. R. Penn, *Surface and Interface Analysis* 17 (1991) 911.
- [63] B. Kim, J. Chen, J. L. Erskine, W. N. Mei, and C. M. Wei, *Phys. Rev. B* 48 (1993) 4735.
- [64] E. D. Tober, R. X. Ynzunza, F. J. Palomares, Z. Wang, Z. Hussain, M. A. Van Hove, and C. S. Fadley, *Phys. Rev. Lett.* 79 (1997) 2085.
- [65] C. Schmidthals, D. Sander, A. Enders, and J. Kirschner, *Surf. Sci.* 417 (1998) 361.
- [66] J. Malzbender, M. Przybylski, J. Giergiel, and J. Kirschner, *Surf. Sci.* 414 (1998) 187.
- [67] N. D. Shinn, C. H. F. Peden, K. L. Tsang, and P. J. Berlowitz, *Physica Scripta* 41 (1990) 607.
- [68] M. J. Gladys, G. Jackson, J. E. Rowe, and T. E. Madey, *Surf. Sci.* 544 (2003) 193.
- [69] B. Kim, N. D. Shinn, and J. L. Erskine, *Journal of the Korean Physical Society* 30 (1997) 625.
- [70] I. G. Batirev, W. Hergert, P. Rennert, V. S. Stepanyuk, T. Oguchi, A. A. Katsnelson, J. A. Leiro, and K. H. Lee, *Surf. Sci.* 417 (1998) 151.
- [71] X. Qian and W. Hübner, *Phys. Rev. B* 60 (1999) 16192.
- [72] D. Spišák and J. Hafner, *Phys. Rev. B* 70 (2004) 195426.
- [73] H. L. Meyerheim, D. Sander, R. Popescu, J. Kirschner, P. Steadman, and S. Ferrer, *Phys. Rev. B* 64 (2001) 045414.

- [74] G. L. Kellogg and P. J. Feibelman, Phys. Rev. Lett. 64 (1990) 3143.
- [75] C. Chen and T. T. Tsong, Phys. Rev. Lett. 64 (1990) 3147.
- [76] G. L. Kellogg and A. F. Voter, Phys. Rev. Lett. 67 (1991) 622.
- [77] G. L. Kellogg, A. F. Wright, and M. S. Daw, J. Vac. Sci. Technol. A 9 (1991) 1757.
- [78] G. L. Kellogg, Phys. Rev. Lett. 76 (1996) 98.
- [79] T. T. Tsong, Phys. Rev. B 6 (1972) 417.
- [80] T. T. Tsong, Phys. Rev. Lett. 31 (1973) 1207.
- [81] H.-W. Fink, K. Faulian, and E. Bauer, Phys. Rev. Lett. 44 (1980) 1008.
- [82] T. T. Tsong and R. Casanova, Phys. Rev. B 24 (1981) 3063.
- [83] H.-W. Fink and G. Ehrlich, Phys. Rev. Lett. 52 (1984) 1532.
- [84] H.-W. Fink and G. Ehrlich, Surf. Sci. 150 (1985) 419.
- [85] H.-W. Fink and G. Ehrlich, J. Chem. Phys. 81 (1984) 4657.
- [86] F. Watanabe and G. Ehrlich, Phys. Rev. Lett. 62 (1989) 1146.
- [87] F. Watanabe and G. Ehrlich, J. Chem. Phys. 95 (1991) 6075.
- [88] F. Watanabe and G. Ehrlich, J. Chem. Phys. 96 (1992) 3191.
- [89] C. Park, E. Bauer, and H. Poppa, Surf. Sci. 154 (1985) 371.
- [90] M. L. Merrick, W. Luo, and K. A. Fichthorn, Progress in Surface Science 72 (2003) 117.
- [91] D. Sander, A. Enders, and J. Kirschner, Europhys. Lett. 45 (1999) 208.
- [92] D. Sander, C. Schmidthals, A. Enders, and J. Kirschner, Phys. Rev. B 57 (1998) 1406.
- [93] R. C. Longo, V. S. Stepansuk, and J. Kirschner, J. Phys.: Condens. Matter 18 (2006) 9143.
- [94] S. J. Koh and G. Ehrlich, Phys. Rev. B 60 (1999) 5981.
- [95] M. Bode, S. Krause, L. Berbil-Bautista, S. Heinze, and R. Wiesendanger, Surf. Sci. 601 (2007) 3308.
- [96] P. Hyldgaard and M. Persson, J. Phys.: Condens. Matter 2000 L13.
- [97] W. L. Jolly and D. N. Hendrickson, J. Am. Chem. Soc. 92 (1970) 1863.
- [98] I. Stensgaard, L. C. Feldman, and P. J. Silverman, Phys. Rev. Lett. 42 (1979) 247.
- [99] D. M. Riffe, G. K. Wertheim, and P. H. Citrin, Phys. Rev. Lett. 65 (1990) 219.
- [100] H. L. Meyerheim, D. Sander, R. Popescu, J. Kirschner, O. Robach, S. Ferrer, and P. Steadman, Phys. Rev. B 67 (2003) 155422.
- [101] P. H. Citrin and G. K. Wertheim, Phys. Rev. B 27 (1983) 3176.